

A Hybrid Energy System Using Cascaded H-bridge Converter

Hui Li¹, Zhong Du², Kaiyu Wang¹, Leon M. Tolbert³, Danwei Liu¹

¹Dept. of ECE, Florida State University, Tallahassee, FL32310, hli@caps.fsu.edu

²Dept. of ECE, North Carolina State University, Raleigh, NC 27695, zdu@ncsu.edu

³Dept. of ECE, The University of Tennessee, Knoxville, TN 37996-2100, tolbert@utk.edu

Abstract*— Different circuit configurations have been researched to combine clean energy sources and energy storage elements. This paper proposes a hybrid energy system to integrate the variable-speed wind turbine, fuel cell, and battery using a cascaded H-bridge converter. One of the advantages of this topology is that it still can obtain the regulated output voltage if one or more energy sources are diminished. In addition, the topology can be easily extended to connect more sources without increasing the circuit and control complexity; therefore, it is beneficial for distributed energy generation. Different operation modes are analyzed in detail. The control schemes were developed to extract maximum wind power and charge/discharge the battery with fast dynamics. The simulation and experimental results are provided to confirm the theoretical analysis.

Keywords - hybrid energy system, cascaded multilevel converter, single dc source

I. INTRODUCTION

As different energy generation technologies become mature, the power generation systems will employ various forms of energy generation, storage, and transmission. The power from hybrid energy systems can be combined on the dc side or ac side through different power conversion configurations [1-5]. A traditional approach to combine power on the ac side is through a multi-phase transformer, shown in Fig. 1. The usage of multi-phase transformer has the following disadvantages: (1) They are the most expensive equipment in the system; (2) They produce about 50% of the total losses of the system; (3) They occupy up to 40% of the total system's real estate; (4) They cause difficulties in control due to dc magnetizing and surge

overvoltage problems resulting from saturation of the transformer in transients; and (5) They are prone to failure [6].

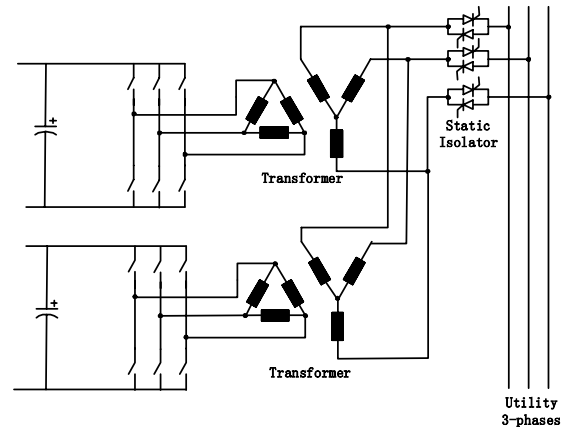


Fig. 1. Hybrid energy system where power is combined on the ac side through a transformer.

In this paper, the outputs from different power sources are integrated on the ac side by a cascaded H-bridge inverter instead of a transformer. The topology can achieve regulated output voltage at a single source if the rest of energy sources are diminished, resulting in increased robustness. Another advantage is the topology can be easily extended to connect more sources without increasing the circuit and control complexity; therefore, it is beneficial for distributed energy generation and high power applications.

II. OPERATION PRINCIPLE

Fig. 2 shows the topology applied to a hybrid energy system integrating the variable-speed wind turbine, fuel cell, and battery as an energy storage element. As shown in Fig. 2, the speed of the generator is controlled through a PWM rectifier to extract the maximum wind energy from the wind turbine. A battery is used as an energy storage element to compensate the stochastic characteristics of wind energy. The ac output of the fuel cell energy source and the ac output of wind turbine - generator system can be combined

* This work was supported by funding under U.S. Department of Energy, Office of Electricity Delivery and Energy Reliability, Award number DE-FG02-05CH11292.

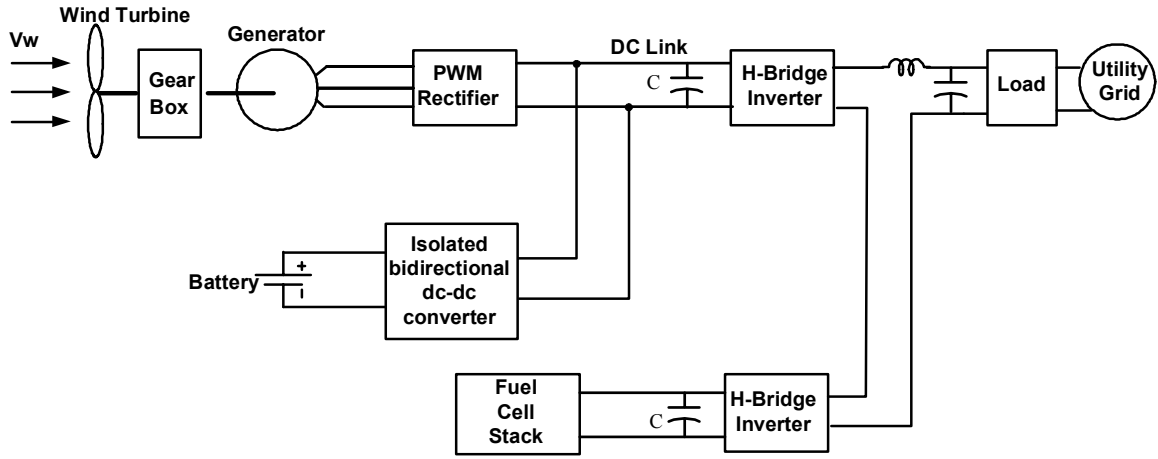


Fig. 2. Proposed hybrid energy system using cascaded H-bridge converters.

in series using a cascaded H-bridge inverter to provide desired power to the load and to the utility grid even if only one source is available and the others are diminished.

A. Operation modes of cascaded inverter

Fig. 2 can be simplified as shown in Fig. 3 where Energy Source 1 represents the wind turbine with battery and Energy Source 2 is the fuel cell stack. V_{dc1} can be assumed to be constant due to the control of the bidirectional dc-dc converter. V_{dc2} can be variable since the fuel cell is connected to the dc bus directly.

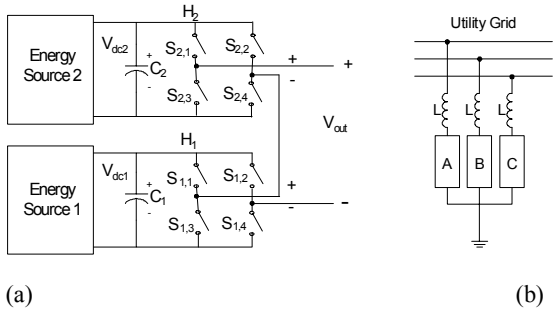


Fig. 3. Simplified hybrid energy system using cascaded H-bridge topology (a) single phase, (b) three-phase.

There are three operation modes for the proposed hybrid energy system: (I) Energy Source 1 standalone mode; (II) Energy Source 2 standalone mode; and (III) mixed mode of Energy Source 1 and Energy Source 2.

To analyze mode I, a dc source is assumed to be connected to the first H-bridge (H_1) with voltage V_{dc} , a capacitor is connected to the second H-bridge (H_2) with capacitor voltage to be held at V_c . For this example, suppose $V_c = V_{dc}/2$. By applying a fundamental switching scheme, the possible combinations of the two H-bridges that can generate 7-level equal step output voltage are shown in

Table I and Fig. 4. From Table I, it can be seen that there are two possible ways to generate $-V_{dc}/2$ and $V_{dc}/2$. One can be used to charge the capacitor while the other can be used to discharge the capacitor. The criteria required for this capacitor balancing scheme is that (1) the desired capacitor voltage is less than the dc source voltage, (2) the capacitance value is chosen large enough so that the variation of its voltage around its nominal value is small (generally, one can choose the capacitor-load time constant to be greater than 10 times of the fundamental cycle time), and (3) the capacitor charging energy is greater than the capacitor discharge energy in a cycle. The operation principles of mode II can be derived similarly.

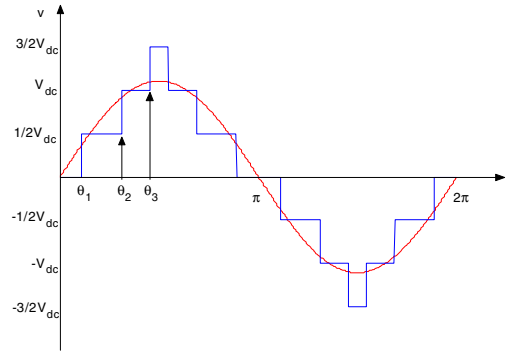


Fig. 4. 7-level equal step output voltage waveform.

Table I. Output voltages for an equal 7-level converter

	v_1	v_2	$v = v_1 + v_2$
$0 \leq \theta < \theta_1$	0	0	0
$\theta_1 \leq \theta < \theta_2$	0	$V_{dc}/2$	$V_{dc}/2$
$\theta_1 \leq \theta < \theta_2$	V_{dc}	$-V_{dc}/2$	$V_{dc}/2$
$\theta_2 \leq \theta < \theta_3$	V_{dc}	0	V_{dc}
$\theta_3 \leq \theta < \pi/2$	V_{dc}	$-V_{dc}/2$	$3V_{dc}/2$

There are two situations of mode III. For the purposes of discussion, $V_{dc1} > V_{dc2}$ is assumed. If the situation is reversed, the control situation is similar.

(1) Situation 1: Energy Source 1 and Energy Source 2 both have enough available power to maintain the dc bus voltages V_{dc1} and V_{dc2} near constant. The cascaded H-bridge converter produces 7 voltage levels $-(V_{dc1}+V_{dc2})$, $-V_{dc1}$, $-V_{dc2}$, 0 , V_{dc2} , V_{dc1} , $V_{dc1}+V_{dc2}$. No power transferring occurs between H₁ bridge and H₂ bridge.

(2) Situation 2: Energy Source 1 has enough available power to maintain the dc bus voltages V_{dc1} near constant; the available power of Energy Source 2 cannot maintain the dc bus voltages V_{dc2} as required. The converter output 9 voltage levels $-(V_{dc1}+V_{dc2})$, $-(V_{dc1}-V_{dc2})$, $-V_{dc1}$, $-V_{dc2}$, 0 , V_{dc2} , V_{dc1} , $V_{dc1}-V_{dc2}$, $V_{dc1}+V_{dc2}$. Power is transferred from H₁ bridge to H₂ bridge to maintain H₂ bridge dc bus to be V_{dc2} . Energy Source 2 charges capacitor C_2 during $-(V_{dc1}-V_{dc2})$ and $(V_{dc1}-V_{dc2})$ period to maintain a near constant dc bus voltage V_{dc2} . Generally, in such a situation, the charging time decides the ratio of the output power between energy source 1 and energy source 2. In addition, during the duration when voltage levels $-(V_{dc1}-V_{dc2})$ and $(V_{dc1}-V_{dc2})$ are produced, Energy Source 1 and Energy Source 2 can charge capacitor C_2 simultaneously.

The modulation index in this cascaded system is defined as:

$$m = \frac{v_f \pi}{2v_{dc}} \quad (1)$$

where v_f is the fundamental magnitude of the output voltage. The modulation index m with two separate dc sources can operate in the region of $0 \leq m \leq 2.52$ [7]. The cascaded inverter with a single dc source cannot achieve the same range. The higher modulation index means a higher output voltage, resulting in the increased load current. The electric charge on the capacitor drawn by the load cannot be compensated by the dc source charging process, so the normal operation cannot be maintained because of the capacitor voltage drop.

In order to find the modulation index range, the variation of the electric charge on the capacitor must be studied first. In the positive half cycle, it can be expressed as

$$Q = \frac{1}{\omega} \int_0^{\pi} i(\theta) S_2(\theta) d\theta, \quad (2)$$

where i is the output current, and ω is the radian frequency. $S_2(\theta)$ here is the switching function for the H-bridge converter with capacitor. The value $Q > 0$ means the

total electric charge on the capacitor is decreasing, and $Q < 0$ means the opposite way. Equation (2) can be rewritten as the following formula considering the interval where $S_2(\theta) = 0$:

$$Q = \frac{1}{\omega} \left[\int_{\theta_1}^{\theta_2} i(\theta) S_2(\theta) d\theta + \int_{\theta_3}^{\pi-\theta_3} i(\theta) S_2(\theta) d\theta + \int_{\pi-\theta_2}^{\pi-\theta_1} i(\theta) S_2(\theta) d\theta \right] \quad (3)$$

This unified equation can be applied to several special cases to solve the corresponding modulation index range.

- *Pure resistive load*

For a pure resistive load, the output current is proportional to the output voltage. In the interval $\theta_3 \leq \theta \leq \pi-\theta_3$, the capacitor is discharged by the load current, so the switching function is chosen to be -1 in the intervals $\theta_1 \leq \theta \leq \theta_2$ and $\pi-\theta_2 \leq \theta \leq \pi-\theta_1$ to compensate the loss. In this case, (3) can be formulated as

$$Q = \frac{1}{\omega R} \left[-\frac{1}{2} v_{dc} (\theta_2 - \theta_1) + \frac{3}{2} v_{dc} (\pi - 2\theta_3) - \frac{1}{2} v_{dc} (\theta_2 - \theta_1) \right] \quad (4)$$

where R is the load resistance. From the previous discussion, the capacitor voltage is maintained only if $Q \leq 0$. The switching angle must satisfy the following inequality derived from (4):

$$3\pi - 6\theta_3 - 2\theta_2 + 2\theta_1 \leq 0$$

The modulation index range for a pure resistive load is therefore: $0 \leq m \leq 1.4$

- *Inductive load*

Assume the high frequency harmonics are filtered by the inductive load, the load current can be regarded as a sinusoidal waveform with the fundamental frequency, and it lags the voltage by phase angle α , shown in Fig. 5.

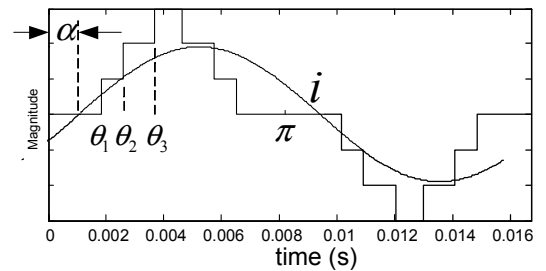


Fig. 5. Induction machine load current

Equation (3) becomes (5):

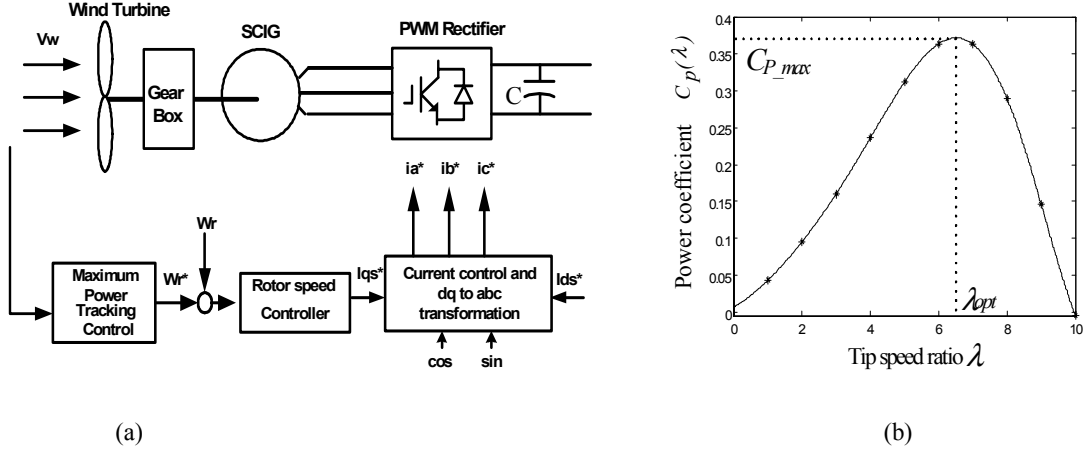


Fig. 6. (a) The control block diagram of wind turbine-generator system, (b) power coefficient vs. tip speed ratio.

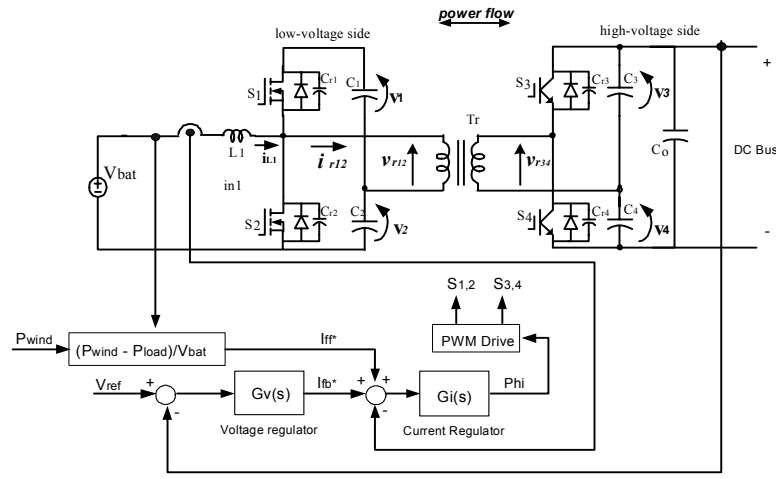


Fig. 7. Energy storage interface with dc bus using isolated bidirectional dual-half-bridge dc-dc converter.

$$\begin{aligned}
 Q &= \frac{1}{\omega} \left[\int_{\theta_1}^{\theta_2} I \sin(\theta - \alpha) S_2(\theta) d\theta \right. \\
 &+ \int_{\theta_3}^{\pi - \theta_3} I \sin(\theta - \alpha) S_2(\theta) d\theta \\
 &\left. + \int_{\pi - \theta_2}^{\pi - \theta_1} I \sin(\theta - \alpha) S_2(\theta) d\theta \right], \quad (5)
 \end{aligned}$$

where I is the peak value of the current. The switching function here is again set to charge the capacitor, and (5) is calculated as:

$$\begin{aligned}
 Q &= \frac{I}{\omega} [\cos(\theta_2 - \alpha) - \cos(\theta_1 - \alpha) + \cos(\theta_3 + \alpha) \\
 &+ \cos(\theta_3 - \alpha) + \cos(\theta_2 + \alpha) - \cos(\theta_1 + \alpha)] \quad (6) \\
 &= \frac{2I \cos \alpha}{\omega} [\cos \theta_2 - \cos \theta_1 + \cos \theta_3],
 \end{aligned}$$

where $\frac{2I \cos \alpha}{\omega} > 0$, since $0 < \alpha < \pi/2$.

Now the triangle inequality can be found as

$$\cos \theta_2 - \cos \theta_1 + \cos \theta_3 \leq 0 \quad (7)$$

The modulation index range satisfying (7) is $0 \leq m \leq 1.54$.

B. Control of wind power and energy storage element

The operation principles of varied-speed wind turbine with battery are described in Fig. 6 and Fig. 7. Fig. 6 (a) is a control block diagram of variable-speed wind turbine system where the rotor speed reference of the generator is designed to extract the maximum power from the wind turbine at a certain wind speed:

$$\omega_r^* = \lambda_{opt} \frac{V_w}{r_m} \quad (8)$$

where V_w is wind speed, r_m is turbine radius, and λ is the tip speed ratio, λ_{opt} is the optimal λ of the maximum power coefficient. A typical power coefficient curve versus tip speed ratio of wind turbine is shown in Fig. 6(b).

Fig. 7 shows the control block diagram of battery interfaced with dc bus using an isolated bidirectional dual half bridge dc-dc converter. The high frequency transformer provides the electric isolation and voltage boost on the high voltage side (dc link). The converter works in buck mode to charge the battery and boost mode to discharge the battery. Under normal operation, the dc-dc converter is controlled to regulate the dc voltage to facilitate the flow of energy. A

double loop control system with power feedforward compensation is designed to achieve superior dynamic performance. The outer voltage loop detects dc link voltage change and generates current reference I_{fb}^* through a voltage regulator. The feedforward current reference is calculated by:

$$I_{ff}^* = (P_{wind} - P_{load}) / V_{bat} \quad (9)$$

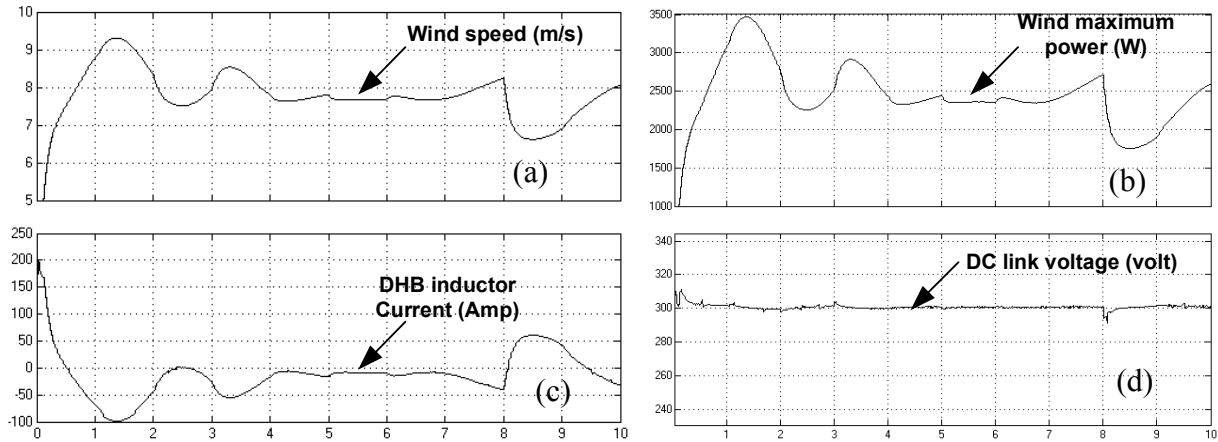


Fig. 8. The simulated performance of wind turbine-battery system (a) changing wind speed, (b) the extracted maximum wind power, (c) the input current of dual-half-bridge (DHB) dc-dc converter, and (d) the dc link voltage of H_1 with battery voltage as 12 V, the desired dc link voltage is 300 V.

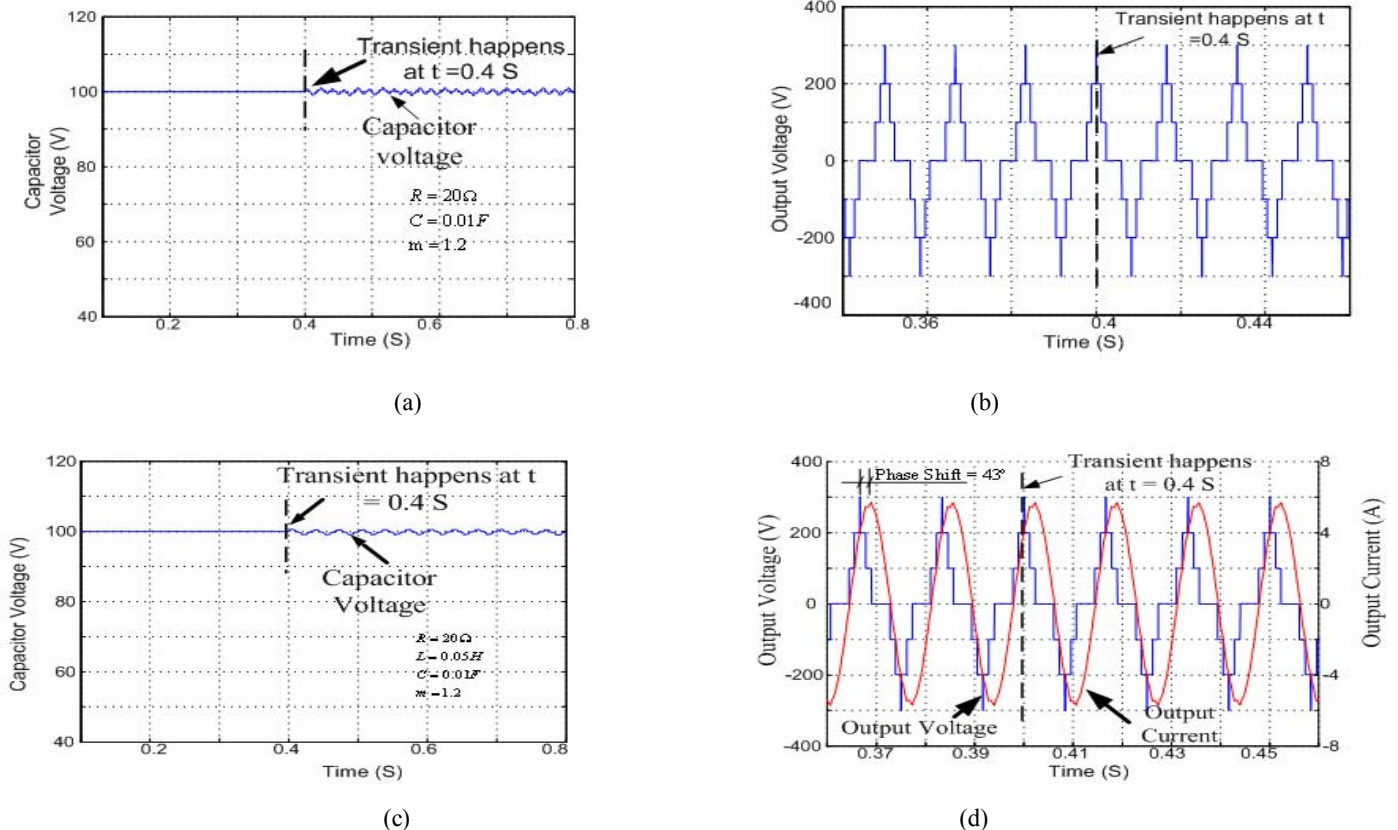
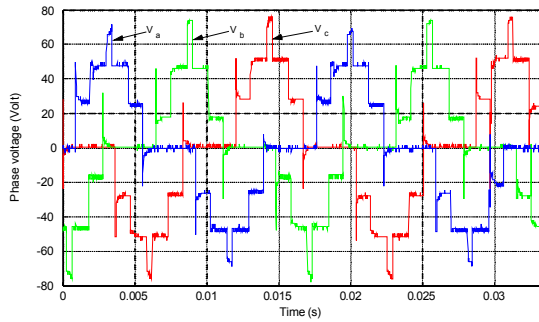
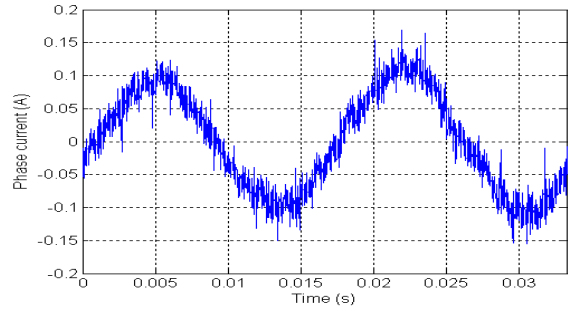


Fig. 9. The simulated operation mode of hybrid energy system (a) capacitor voltage with resistive load, (b) output voltage with resistive load, (c) capacitor voltage with inductive load, and (d) output voltage and current with inductive load when $V_{dc1}=200V$, $V_{dc2}=100V$.



(a)



(b)

Fig. 10. The experimental results of mixed operation mode of Energy Source 1 and 2 when $V_{dc1}=48V$ and $V_{dc2}=24V$ (a) three phase output voltage, and (b) single phase output current

P_{wind} is the wind power in accordance with wind speed. P_{load} is nominal power of the load. V_{bat} is the detected battery voltage, and in this case, the battery voltage variation could be also compensated by feed forward control. In addition, soft switching is achievable for this converter to increase the efficiency.

III. PERFORMANCE VERIFICATION

The control performance of a wind turbine with battery is simulated with parameters listed in Appendix. The simulated performance is shown in Fig. 8. The dc-dc converter is controlled to regulate the dc link voltage by charging and discharging the battery.

Fig. 9 shows the simulated performance of different operation modes of the cascaded inverter at resistive load ((a)-(b)) and inductive load ((c)-(d)). The system is initially working at two separate dc sources, i.e., $V_{dc1}=200V$, $V_{dc2}=100V$. At $t=0.4s$, V_{dc2} is diminished and only a 10mF capacitor is left to provide the regulated output voltage with V_{dc1} . The results show the output voltages have not changed before and after the transients. Fig. 10 shows the experimental results of output voltage and current when Energy Source 1 and 2 are operated in mixed operation mode with $V_{dc1}=24V$ and $V_{dc2}=48V$.

IV. CONCLUSION

This paper studies a cascaded hybrid energy system that can operate with separate dc sources or a single dc source by controlling the charge and discharge balance of a capacitor. The balance voltage control method can be applied to any type of load. The effect of modulation index range with a resistive load and an inductive load has been analyzed. The

advantage of this power configuration and the corresponding control scheme is to improve the system survivability and power quality. The simulation and experimental results are provided to verify the analysis.

REFERENCES

- [1] N. Kato, K. Kurozumi, N. Susuld, S.Muroyama, "Hybrid power-supply system composed of photovoltaic and fuel-cell systems," *Proceeding of International Telecommunications Energy Conference*, Oct. 2001, pp. 631 - 635.
- [2] Z.Chen, Y. Hu, "A hybrid generation system using variable speed wind turbines and diesel units," *Annual Conference of the IEEE Industrial Electronics Society*, vol. 2, Nov. 2003, pp. 2729 - 2734.
- [3] W. Carter, B. M. Diong, "Model of a regenerative fuel cell-supported wind turbine ac power generating system," *Proceeding of IEEE Industry Application Conference*, Oct. 2004, vol. 4, pp. 2778-2785.
- [4] K. Strunz, E.K.Brock, "Hybrid plant of renewable stochastic source and multilevel storage for emission-free deterministic power generation," *Proceeding of CIGRE/IEEE PES International Symposium*, Oct. 2003, pp. 214 - 218, Oct. 2003.
- [5] K. Rajashekara, "Hybrid fuel-cell strategies for clean power generation," *IEEE Transactions on Industry Applications*, vol. 41, no. 3, May/June 2005, pp. 682-689.
- [6] F. Z. Peng, et. al., "A multilevel voltage-Source inverter with separate dc Sources for staic var generation," *IEEE Transactions on Industry Applications*, vol. 32, no. .5, Sept./Oct. 1996, pp. 1130-1138.
- [7] J. Chiasson, L. M. Tolbert, K. McKenzie, Z. Du, "Control of a multilevel converter using resultant theory," *IEEE Transactions on Control System Technology*, vol. 11, no. 3, pp. 345-354, May 2003.
- [8] Z. Du, L. M. Tolbert, J. N. Chiasson, B. Ozpineci, "A cascade multilevel inverter using a single dc power source," *IEEE Applied Power Electronics Conference*, March 19-23, 2006, Dallas, Texas, pp. 426-430.